Proceedings of *RAGtime 20–22, 15–19 Oct., 16–20 Sept., 19–23 Oct., 2018/2019/2020, Opava, Czech Republic*
Z. Stuchlík, G. Török and V. Karas, editors, Silesian University in Opava, 2020, pp. 121–132

The effect of magnetic field on the structure of strange quark star

Fatemeh Kayanikhoo[1,a] and Constança Providência[2]

[1]Nicolaus Copernicus Astronomical Center,
Bartycka 18, 00-716, Warszaw, Poland,
[2]CFisUC, Department of Physics, University of Coimbra, Coimbra, Portugal
[a]fatima@camk.edu.pl

ABSTRACT
The study of the strange quark stars is an interesting subject as they are a new possible type of compact object in extreme conditions. Theoretical studies suggest that the magnetic field inside the compact objects (neutron stars and SQS) may be of the order of $\sim 10^{18}$G. This strong magnetic field can affect the shape, mass, and radius of the compact objects. In the current work, we study the effect of the strong magnetic field on the equation of state and the structure of SQS. We show that the maximum gravitational mass of the SQS increases with increasing the magnetic field. Also, we find that our model corresponds to the 2 solar mass gravitational mass which is predicted for *PSR J1614-2230* and *PSR J0348+0432*. It is notable that the maximum gravitational mass in our model is $\sim 2.5 M_{\odot}$, that is comparable with the value that is predicted by detection of the gravitational wave by LIGO/Virgo collaboration. In addition, the results show that the star has an oblate shape under the effect of the strong magnetic field.

Keywords: Strange quark star – compact objects –magnetic field – quark matter – Landau effect

1 INTRODUCTION

Strange quark stars (SQS) are a possible type of compact object which remains after the end of the life of supermassive stars. After the first explosion of a massive star if the density of matter in the core of the star increases to the values above the nuclear saturation density ($\sim 10^{15}$) the quarks deconfine and a huge amount of energy ($\sim 10^{54}$ erg) released, there is a possibility that this energy leads to the second explosion which is super luminous and is called Quark-Nova (QN). The object which remains after the QN is a SQS (Ouyed et al., 2002; Ouyed and Staff, 2013; Nurmamat et al., 2019). Ouyed, Leahy, and Koning studied *CassiopeiaA* as an excellent candidate for the QN. They showed that the second explosion has happened some days after the supernova and leads to a transition from a neutron star to a quark star (Ouyed et al., 2015).

Compact object like hybrid stars and SQS contain strange quark matter (SQM) that can exist in extreme conditions (high density and temperature, and the strong magnetic fields), therefore the study of these objects has been undertaken by different groups in recent years. These objects are real laboratories to study fundamental physics in extreme conditions. In the current work, we study the effect of strong magnetic fields on the properties of the SQS. Like neutron stars and hybrid stars (the compact objects with a quark core), the SQS may have strong magnetic fields. If a massive star has a high magnetic field, during the core collapse of the supernova the magnetic flux is conserved and the compact object is created with a strong magnetic field. According to the theoretical studies the magnetic field in the core of compact objects reaches $\sim 10^{18}$ G (Lai and Shapiro, 1991; Haensel et al., 1986; Bocquet et al., 1995; Isayev, 2014).

It is notable that the properties of the star are affected by the strong magnetic field. There are several studies on the microscopic and macroscopic properties of compact objects in the presence of the magnetic field. Chatterjee, et al. studied the effect of a strong magnetic field on the EOS and the structure of a neutron star and they showed that the magnetic field breaks the spherical symmetry of neutron star(Chatterjee et al., 2015)

In the current paper, we study the effect of a strong magnetic field on the EOS and the structure of SQS. In the next section, we calculate the EOS of the system consisting of SQM (up, down, and strange quarks) in the presence of the strong magnetic field. In section 3 we study the anisotropic energy-momentum tensor of the system and the structure equations of SQS in a stationary, axisymmetric space-time. In section 4, we report the numerical results and discuss the magnetic field effects. In last section, we summarize and conclude our study.

2 THE EQUATION OF STATE OF STRANGE QUARK MATTER IN THE PRESENCE OF THE STRONG MAGNETIC FIELDS

The system we consider consists of SQM (up, down and strange quarks and an ignorable fraction of electrons $\sim 10^{-3}$). We calculate the EOS of this system by applying the MIT bag model. The Fermi relations by considering the effect of a strong magnetic field, regarding the Landau quantization effect (Mukhopadhyay et al., 2017; Landau and Lifshitz, 1977; Lopes and Menezes, 2015), are given by the following relations.

The single-particle energy density is defined as follows

$$\epsilon_{\rm i} = \left[p_{\rm i}^2 c^2 + m_{\rm i}^2 c^4 \left(1 + 2JB_{\rm D}\right)\right]^{1/2}, \tag{1}$$

where $p_{\rm i}$ and $m_{\rm i}$ are the momentum and the mass of quarks (i represents u, d, s), the Landau levels are denoted by J and the dimensionless magnetic field defined as $B_{\rm D} = B/B_{\rm C}$ ($B_{\rm C} = m_{\rm i}^2 c^3/q_{\rm i}\hbar$, with $q_{\rm i}$ the charge of quark i).

The number density of quarks is obtained as follows

$$\rho = \sum_{J=0}^{J_{\rm max}} \frac{2qB}{h^2 c} g(J) P_{\rm F}(J), \tag{2}$$

where $J_{\rm max}$ is the maximum Landau level ($J_{\rm max} = (\epsilon_{\rm Fmax}^2 - 1)/2m_i c B_D$), $g(J)$ and $P_{\rm F}(J)$ are the degeneracy and Fermi momentum of Jth Landau level. Therefore, the energy density

of SQM in the presence of the strong magnetic field is defined as

$$\varepsilon_{\rm tot} = \sum_{\rm i,j} \varepsilon_{\rm i}^{\rm (j)} + B_{\rm bag}. \tag{3}$$

The bag constant is denoted by $B_{\rm bag}$ and the kinetic energy density by $\varepsilon_{\rm i}$ ($j = +, -$ shows the spin up and apin down particles). The kinetic energy density is defined as follows

$$\varepsilon_{\rm i}^{\rm (j)} = \frac{2B_D}{(2\pi)^2\lambda^3} m_{\rm i} c^2 \sum_{J=0}^{J_{\rm max}} g_{\rm J}(1+2JB_{\rm D})\eta\left(\frac{X_{\rm F}^{\rm (j)}}{(1+2JB_{\rm D})^{1/2}}\right), \tag{4}$$

where

$$\eta(x) = \frac{1}{2}\left[x\sqrt{1+x^2} + \ln\left(x\sqrt{1+x^2}\right)\right] \tag{5}$$

and

$$x = \frac{X_{\rm F}^{\rm (j)}}{(1+2JB_{\rm D})^{1/2}} \tag{6}$$

and

$$X_{\rm F}^{\rm (j)} = (\epsilon_{\rm F}^{\rm (j)2} - 1 - 2JB_{\rm D})^{1/2}. \tag{7}$$

To calculate the energy density of SQM in a zero magnetic field, we calculate the value of number density and energy density when $J_{\rm max} \to \infty$.

The bag constant $B_{\rm bag}$ is defined with a Gaussian relation

$$B_{\rm bag}(\rho) = \bar{B}_\infty + \left(\bar{B}_0 - \bar{B}_\infty\right)\exp\left(-\beta\left(\frac{\rho}{\rho_0}\right)^2\right). \tag{8}$$

In above relation $\beta = \rho_0 = 0.17\,{\rm fm}^{-3}$, and $\bar{B}_0 = \bar{B}(\rho_0)$ is equal to $400\,{\rm MeV/fm}^3$. Also, $\bar{B}_\infty$ depends the parameter $\bar{B}_0$ and is obtained by the LOCV method (Heinz and Jacob, 2000).

The pressure of system is given by

$$P(\rho) = \rho\left(\frac{\partial\varepsilon_{\rm tot}}{\partial\rho}\right) - \varepsilon_{\rm tot}. \tag{9}$$

The EOS is plotted in Fig. 1 in the presence of magnetic fields 10^{17} G and 10^{18} G and absence of magnetic field ($B = 0$). We can see the effect of magnetic field on the EOS in comparison with $B = 0$. Also, the figure shows that the difference between the curves of different magnetic fields is not significant.

3 THE STRUCTURE EQUATIONS

In this section, we briefly present the Einstein field equations within 3+1 formalism in a stationary, axisymmetric space-time (Chatterjee et al., 2015).

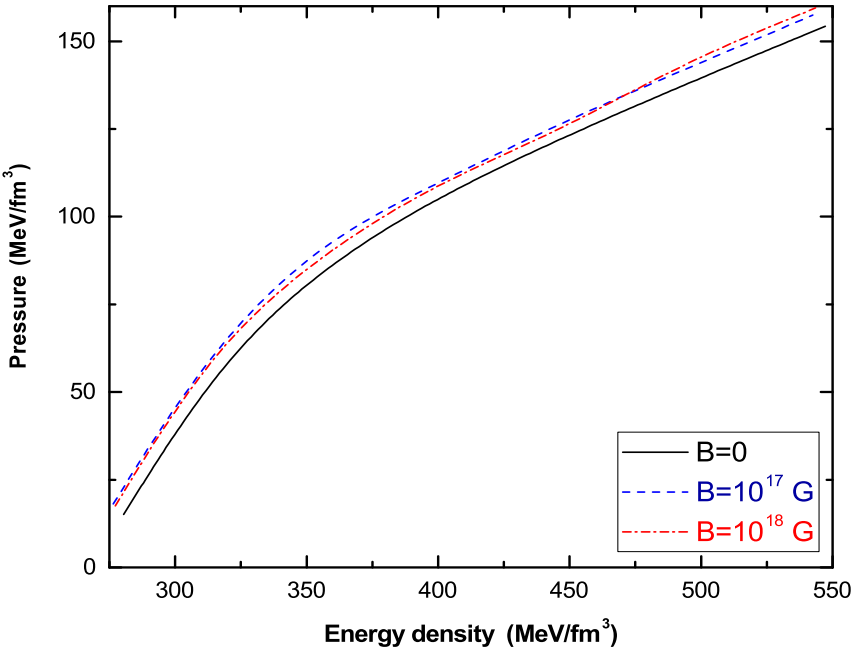

Figure 1. The pressure as a function of the energy density of SQM in the presence and absence of magnetic field.

The metric is given by

$$ds^2 = -N^2dt^2 + A^2(dr^2 + r^2d\theta^2) + \lambda^2 r^2 \sin^2(\theta)(d\phi - N^\phi dt)^2, \tag{10}$$

where N, A, λ, and N^ϕ are function of (r, θ). By applying 3+1 formalism we will have a set of four elliptic partial differential equations

$$\Delta_3 = 4\pi A^2(E^T + S_r^r + S_\theta^\theta + S_\phi^\phi) + \frac{\lambda^2 r^2 \sin^2(\theta)}{2N^2}\delta N^\phi \delta N^\phi - \delta\nu\delta(\nu + \beta), \tag{11}$$

$$\Delta_2[\alpha + \nu] = 8\pi A^2 S_\phi^\phi + \frac{3\lambda^2 r^2 \sin^2(\theta)}{4N^2}\delta N^\phi \delta N^\phi - \delta\nu\delta\nu, \tag{12}$$

$$\Delta_2[(N\lambda - 1)r\sin(\theta)] = 8\pi N A^2 \lambda r \sin(\theta)\left(S_r^r + S_\theta^\theta\right) \tag{13}$$

and

$$\left[\Delta_3 - \frac{1}{r^2\sin^2(\theta)}\right]\left(N^\phi r\sin(\theta)\right) = -16\pi\frac{NA^2}{\lambda^2}\frac{J^\phi}{r\sin(\theta)} + r\sin(\theta)\delta N^\phi\delta(\nu - 3\beta), \tag{14}$$

where $\nu = \ln N$, $\alpha = \ln A$, $\beta = \ln \lambda$, and J^{ϕ} is electromagnetic current. In the above equations, E^T, and S^i_j are total energy and stress, respectively. The notations Δ_2 and Δ_3 are introduced

$$\Delta_2 = \frac{\delta^2}{\delta r^2} + \frac{1}{r}\frac{\delta}{\delta r} + \frac{1}{r^2}\frac{\delta^2}{\delta \theta^2}, \tag{15}$$

$$\Delta_2 = \frac{\delta^2}{\delta r^2} + \frac{2}{r}\frac{\delta}{\delta r} + \frac{1}{r^2}\frac{\delta^2}{\delta \theta^2} + \frac{1}{r^2 \tan(\theta)}\frac{\delta}{\delta \theta}. \tag{16}$$

The the matter properties affects the structure of star through the energy-momentum tensor $T^{\mu\nu}$. In the presence of the magnetic field by considering the interaction of the electromagnetic field with the matter (magnetization), the energy-momentum tensor is given by

$$\begin{aligned} T^{\mu\nu} =& (\varepsilon + P)u^{\mu}u^{\nu} + Pg^{\mu\nu} + \frac{M}{B}\left[b^{\mu}b^{\nu} - (b.b)\left(u^{\mu}u^{\nu} + g^{\mu\nu}\right)\right] \\ &+ \frac{1}{\mu_0}\left[-b^{\mu}b^{\nu} + (b.b)\left(u^{\mu}u^{\nu} + \frac{1}{2}g^{\mu\nu}\right)\right], \end{aligned} \tag{17}$$

where the two first terms are the perfect fluid contribution, the third term is the magnetization contribution and the last term is the pure magnetic field contribution to the energy-momentum tensor. In the Eq. (17), ε is the energy density, P is the pressure of the perfect fluid, u^{μ} is the fluid 4-vector, $g^{\mu\nu}$ is the metric coefficient, B is the magnetic field, and b^{μ} is the magnetic field 4-vector. In the above relation, M is the scalar quantity which is defined as follows

$$M := \mu_0 \frac{m_{\mu}}{b_{\mu}}, \tag{18}$$

where m_{μ} is magnetization 4-vector. Here the magnetic field points in z-direction and we considered a non-rotating star. We can rewrite the energy-momentum tensor in the well-known form

$$T^{\mu}_{\nu} = \mathrm{diag}\left(\varepsilon + \frac{B^2}{2\mu_0}, P - MB + \frac{B^2}{2\mu_0}, P - MB + \frac{B^2}{2\mu_0}, P - \frac{B^2}{2\mu_0}\right). \tag{19}$$

The energy-momentum tensor Eq. (19) shows that the magnetization term reduces the total pressure of the star. It is also clear that the magnetic field reduces the parallel pressure but the perpendicular pressure is increasing by increasing the magnetic field. Consequently, the star will be deformed in the presence of a strong magnetic field.

In the next section we show the results of solving the equations by applying the LORENE (*Lorene/Codes/Mag _ eos _ star*) and using the defined EOS in the previous section (Gourgoulhon et al., 2016).

4 THE NUMERICAL RESULTS

In this section, we investigate the effect of the magnetic field on the structure of SQS by varying the current function k_0 defined through $j^{\phi} = \Omega j^{t} + (\varepsilon + P)k_0$, where Ω is the stellar angular velocity. We study the structure of SQS in two cases,

i) The magnetic field just affects the structure of SQS,

ii) The magnetic field affects the structure and the EOS of SQS.

We have found that in our model the current function can reach 30000. In other words, for $k_0 > 30000$ the SQS is not in a stable configuration.

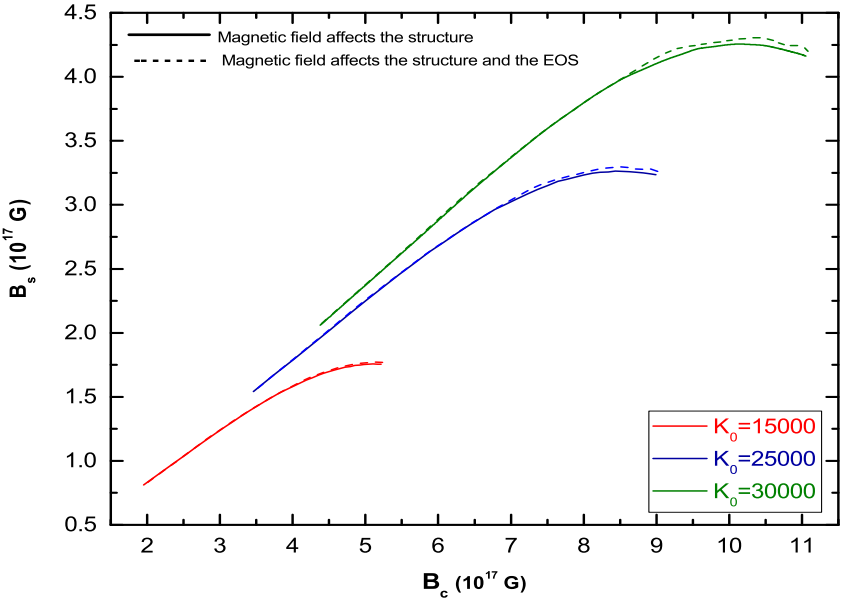

Figure 2. The surface magnetic field at the pole B_s as a function of the central magnetic field B_c.

In Fig. 2, we show the surface magnetic field of SQS in the pole B_s as a function of central magnetic field B_c. It is shown that B_s and B_c increase with increasing the current function. It is also shown that in the lowest value of k_0 the two considered cases cover each other and when $k_0 = 30000$, the difference between the two considered cases (dash lines and solid lines) is non negligible. The figure shows that the maximum central magnetic field is $B_c \sim 10^{18}$ G and that the maximum polar magnetic field at the surface $B_s \sim 4 \times 10^{17}$ G occurs at $k_0 = 30000$.

The gravitational mass $(M_g/M_{\odot})$ versus the central enthalpy H_c is plotted in the top panel of Fig. 3. The enthalpy can be translated to the baryonic density $n_B = (\varepsilon + P)e^{H}$. The figure shows that the gravitational mass increases as a function of central enthalpy in every considered case. The results show that the effect of the magnetic field on the EOS

has a negligible effect on the gravitational mass of SQS. It is shown that M_g increaces with increacing k_0. The maximum gravitational mass is 2.35 $M_\odot$ at $k_0 = 0$ ($k_0 = 0$ means that we are solving the TOV equations) and increaces to 2.48 $M_\odot$ at $k_0 = 30000$.

We have found that our model for the compact objects describes 2 $M_\odot$ stars as it is observed for the pulsars *PSR J1614-2230* ($M = 1.908 \pm 0.016\, M_\odot$) and *PSR J0348+0432* ($M = 2.01 \pm 0.04\, M_\odot$)(Demorest et al., 2010; Zhao, 2015), see Table 1. In addition, it is interesting to notice that the maximum gravitational mass corresponding to the maximum magnetic field in our calculations falls close to the predicted mass of the low mass compact object, with a mass 2.5 to 2.67 $M_\odot$ at 90% confidence, of the compact binary coalescence corresponding to the recent gravitational waves *GW190814* detected by the LIGO/Virgo collaboration. It is predicted at (Abbott et al., 2020).

In the bottom panel of Fig. 3, we show the mass-radius relation of SQS, and in Table1 we give the properties of the maximum mass configurations for different values of k_0, as well as the radius of 1.4 $M_\odot$ and 1.6 $M_\odot$ stars. It is clear that the radius increases with increasing the gravitational mass, when the gravitational mass reaches a certain value, the radius decreases and SQS collapses. In this figure, we show the central magnetic field corresponding to the maximum radius of SQS which increases from 4.60×10^{17} G to 9.15×10^{17} G. Forthermore, one can see the mass-radius relation clearly follows $R \propto M^\alpha$ where $\alpha \sim 3$ which is expected for SQS.

The radius of the maximum mass configuration increases from radius of SQS is 12.13 km for $k_0 = 0$ to 13.16 km at $k_0 = 30000$.

Table 1. The gravitational mass and radius of SQS in different current functions. Results for the maxmium mass configuration and for the $1.4M_\odot$ and $1.6M_\odot$ stars are shown.

k_0	$B_c(10^{17}$ G)	$M_{g,max}(M_\odot)$	R_{max} (km)	$R_{1.4}$ (km)	$R_{1.6}$ (km)
$k_0 = 0$		2.35	12.13	10.74	11.10
$k_0 = 15000$	5.24	2.38	12.35	10.81	11.35
$k_0 = 25000$	9.02	2.43	12.80	11.13	11.59
$k_0 = 30000$	10.60	2.48	13.16	11.33	11.86

In Table 1 we show the values of the maximum gravitational mass and the corresponding radius in the third and fourth columns, respectively. We also give the radius of the stars with gravitation masses of 1.4 $M_\odot$ ($R_{1.4}$) and 1.6 $M_\odot$ ($R_{1.6}$). These results show that our model is compatible with the constraints imposed the *GW170817* analysis, in particular, the following constraints have been obtained $9.9 < R_{1.4} < 13.85$ km (Annala et al., 2018), $8.9 < R_{1.4} < 13.2$ km in (De et al., 2018) and $9.0 < R_{1.4} < 13.6$ km in Tews et al. (2018).

On the other hand, our $R_{1.4M_\odot}$ are within two sigma the predictions obtained from the *NICER* observation of the pulsar *PSR J0030+0451*. Miller and et al have estimated that the pulsar *PSR J0030+0451* has a radius $R_{1.4} = 13.02^{+1.24}_{-1.06}$ km for the gravitational mass $M = 1.44^{+0.15}_{-0.14}\, M_\odot$ within a 68% confidence interval (Miller et al., 2019). A different estimation

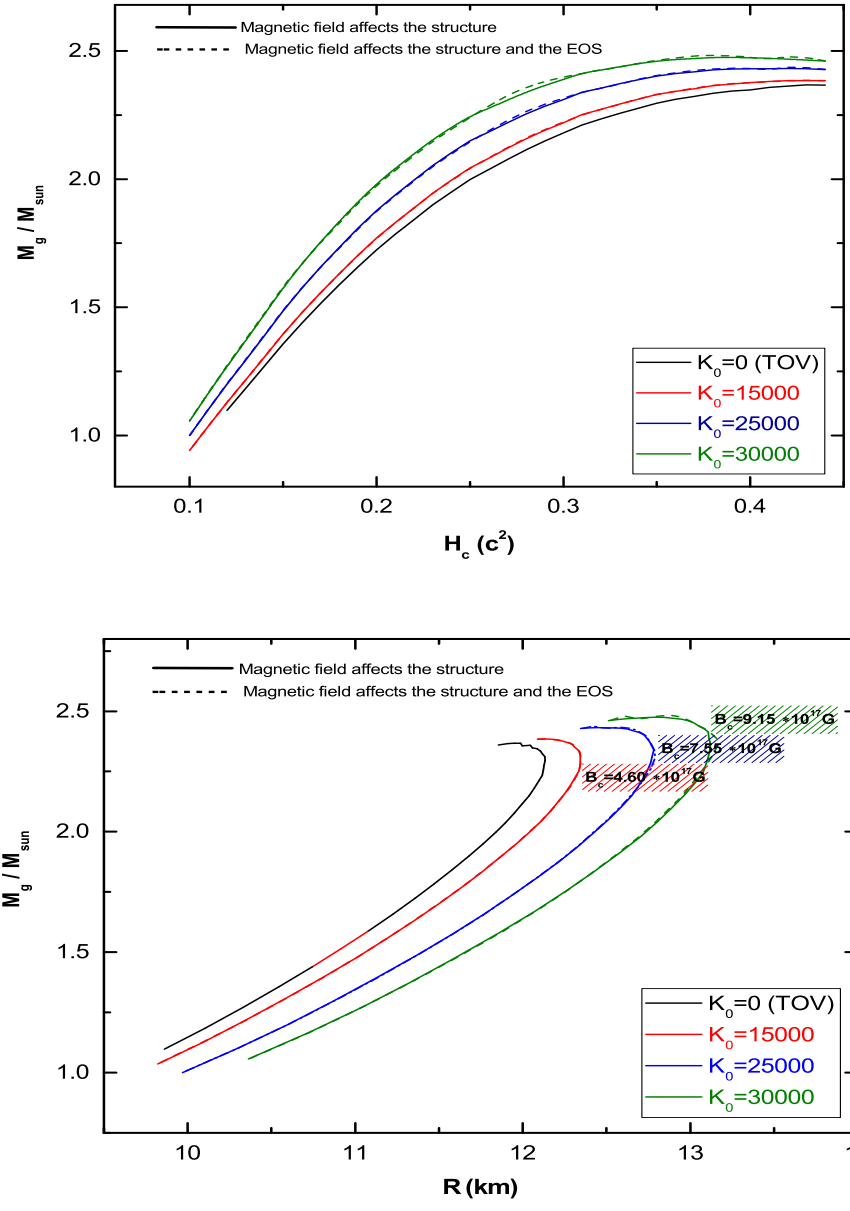

Figure 3. The gravitational mass as a function of central enthalpy (top) and the gravitational mass as a function of circumferential radius (bottom) for different values of the parameter k_0. In the bottom panel, we put the central magnetic field at the maximum radius (the critical point of the curve) in the same color given for each curve.

determined by Riley et al. (Riley et al., 2019) corresponds to a gravitational mass and a radius of $1.34^{+0.15}_{-0.16}\,M_\odot$ and $12.71^{+1.14}_{-1.19}$ km, respectively.

It has also been set a minimum radius of $R_{1.6} \geq 10.7$ for 1.6 $M_\odot$ star from the interpretation that the binary nS merger that gave rise to *GW170817* did not result from a prompt collapse to a black hole (Bauswein et al., 2017, 2019). In our study we have determined that $R_{1.6} > 10.7$ independently of the magnetic field considered. We conclude, therefore, that our model is also compatible with the constraint set on $R_{1.6}$.

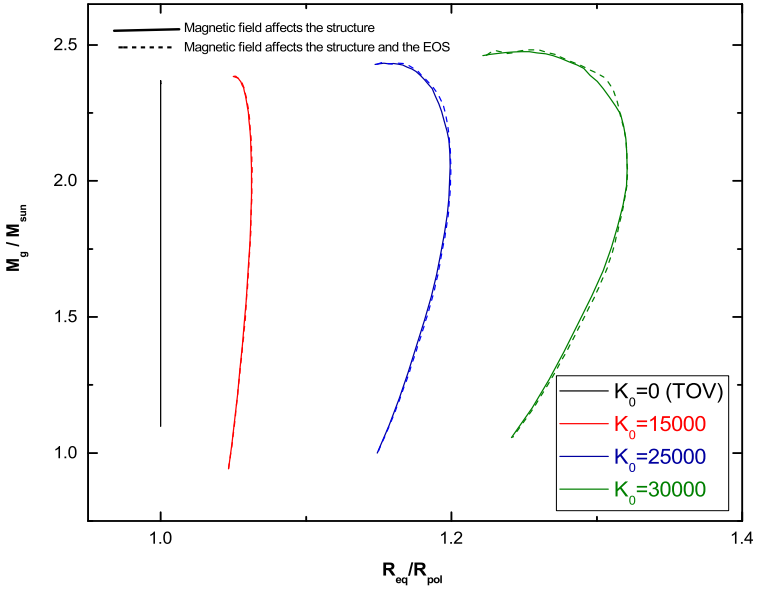

Figure 4. The gravitational mass versus the ratio of the equatorial and polar radius of SQS.

We mentioned in Sec. 3 that the magnetic field affects the shape of SQS as the parallel pressure is reduced and perpendicular pressure is increased according to the energy-momentum tensor Eq. (19). In Fig. 4, The gravitational mass is plotted as a function of $R_{\rm eq}/R_{\rm pol}$. We can see that by solving the TOV equations the SQS is completely in spherical symmetry, the ratio of equatorial and polar radius increases with increasing the current function, and at $k_0 = 30000$ this value reaches to 1.25. It is also clear that the effect of the magnetic field on the EOS does not affect the shape of SQS.

In Fig. 5, the magnetic field lines (top panel) and the enthalpy profile (bottom panel) are plotted in the plane (x, z). The profiles are plotted for the gravitational mass $2.48M_\odot$ and the polar surface magnetic field 4.25×10^{17} G. The bold line in both panels shows the surface of SQS. The magnetic field profile shows how the strong magnetic field can deviate

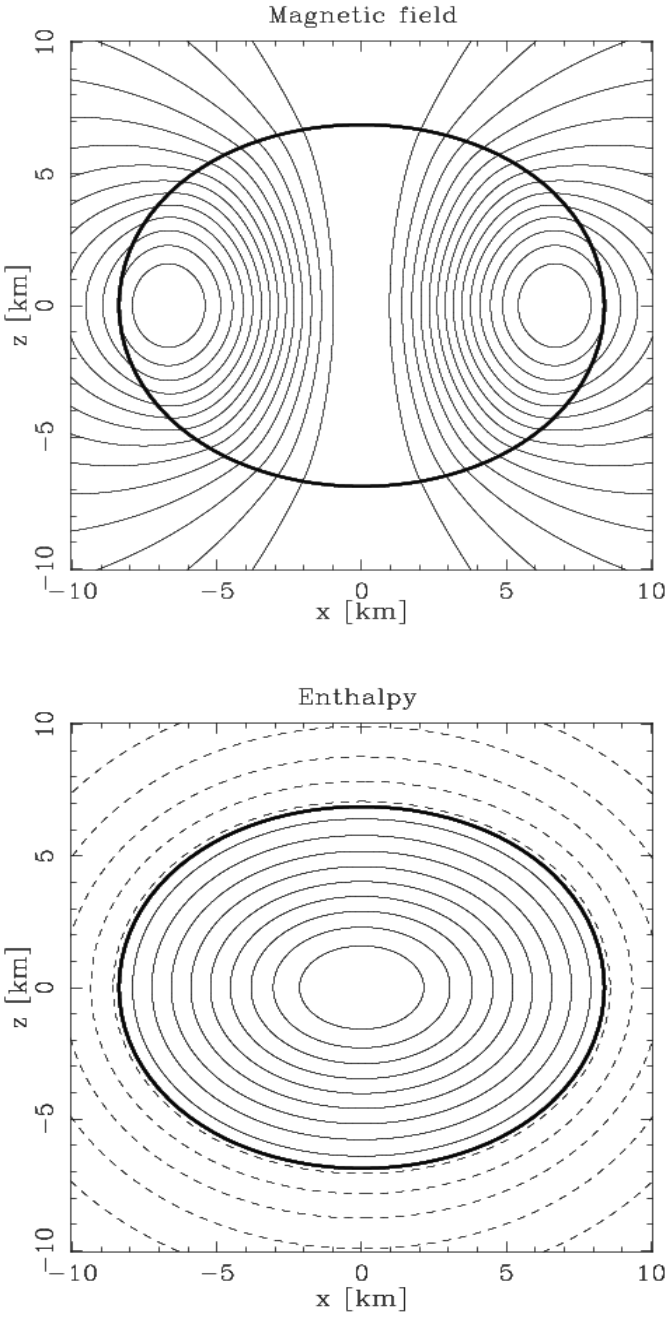

Figure 5. The profile of magnetic field lines (top) and the enthalpy profile (bottom) in meridional plane (x, z) for the maximum value of magnetic field $B_s = 4.25 \times 10^{17}$ G and gravitational mass $M_g = 2.5\, M_\odot$.

the shape of SQS from the spherical symmetry. In the enthalpy profile, the dash lines are negative enthalpy and the solid lines are positive enthalpy inside the SQS.

5 CONCLUSIONS

In this work, we studied the effect of a strong magnetic field on the microscopic and macroscopic properties of SQS. We calculated the EOS of SQM with the Landau quantization effect. To investigate the structure we assumed the stationary, axisymmetric space-time. The microscopic properties of matter affect the structure through the energy-momentum tensor. In the presence of the strong magnetic field, the energy-momentum tensor is in an anisotropic form. It is shown that the parallel and perpendicular pressures are reduced by the magnetization. The magnetic field reduces the parallel pressure and increases the perpendicular pressure.

We have found that the magnetic field in the core of SQS reaches to $\sim 10^{18}$ G where the maximum surface magnetic field at the pole is $\sim 4 \times 10^{17}$ G. The results show that the maximum gravitational mass and radius of SQS increase as the magnetic field becomes stronger and may reach the value 2.48 $M_\odot$ and the radius 13.16 km, respectively, taking the strongest field considered in the present study. This value of gravitational mass is comparable with the predicted, by the LIGO/Virgo collaboration, smallest value for the low mass object associated with the gravitational waves GW190814, in particular, at 90% confidence this compact object should have a mass between 2.5 $M_\odot$ and 2.67 $M_\odot$. This could indicate that this object is a strongly magnetized star. We have also shown that the radius predictions obtained from our model for magnetized and non-magnetized stars with a mass 1.4 $M_\odot$ and 1.6 $M_\odot$ is compatible with the values obtained from several different analysis of the *GW170817*.

It is also clear that the strong magnetic field affects the shape of the star. The strong magnetic field breaks down the spherical symmetry of the star. The ratio of equatorial and polar radius reaches 1.25 in the maximum value of the central magnetic field 10^{18} G.

ACKNOWLEDGEMENTS

This work has been done at the University of Coimbra. I would like to show my gratitude to Ivo Sengo and Dr. Helena Pais for technical assistance with LORENE. I would like to express my very great appreciation to Prof. Wlodek Kluzniak at Nicolaus Copernicus Astronomical Center. Publication supported in part by the Polish NCN grant No. 2019/33/B/ST9/01564.

REFERENCES

Abbott, R., Abbott, T. D., Abraham, S., Acernese, F., Ackley, K., Adams, C., Adhikari, R. X., Adya, V. B. and et al (2020), GW190814: Gravitational Waves from the Coalescence of a 23 Solar Mass Black Hole with a 2.6 Solar Mass Compact Object, *Astrophys. J.*, **896**(2), p. 44.

Annala, E., Gorda, T., Kurkela, A. and Vuorinen, A. (2018), Gravitational-wave constraints on the neutron-star-matter Equation of State, *Phys. Rev. Lett.*, **120**(17), p. 172703.

Bauswein, A., Friedrich, N. U. B., Blaschke, D., Chatziioannou, K. and et al (2019), Equation-of-state Constraints and the QCD Phase Transition in the Era of Gravitational-Wave Astronomy, *AIP Conf. Proc.*, **2127**(1), p. 020013.

Bauswein, A., Just, O., Janka, H. T. and Stergioulas, N. (2017), Neutron-star radius constraints from GW170817 and future detections, *Astrophys. J. Lett.*, **850**(2), p. 34.

Bocquet, M., Bonazzola, S., Gourgoulhon, E. and Novak, J. (1995), Rotating neutron star model with magnetic field, *Astron. Astrophys*, **301**, p. 757.

Chatterjee, D., Elghozi, T., Novak, J. and Oertel, M. (2015), Consistent neutron star models with magnetic-field-dependent equations of state, *Mon. Not. R. Astron. Soc*, **447**(4).

De, S., Finstad, D., Lattimer, J. M., Brown, D. A., Berger, E. and Biwer, C. M. (2018), Tidal Deformabilities and Radii of Neutron Stars from the Observation of GW170817, *Phys. Rev. Lett.*, **121**(9), p. 091102.

Demorest, P. B., Pennucci, T., Ransom, S. M., Roberts, M. S. E. and Hessels, J. W. T. (2010), A two-solar-mass neutron star measured using Shapiro delay, *Nature*, **467**, p. 1081.

Gourgoulhon, E., Grandclement, P., Marck, J. A., Novak, J. and Taniguchi, K. (2016), LORENE: Spectral methods differential equations solver.

Haensel, P., Zdunik, J. L. and Schaeffer, R. (1986), Strange quark stars, *Astron. Astrophys*, **160**(121).

Heinz, U. and Jacob, M. (2000), Evidence for a new state of matter: An assessment of the results from the CERN lead beam programme, *nucl-th/0002042*.

Isayev, A. A. (2014), Absolute stability window and upper bound on the magnetic field strength in a strongly magnetized strange quark star, *Int. J. Mod. Phys. A*, **29**(30).

Lai, D. and Shapiro, L. (1991), Cold equation of state in a strong magnetic field: Effect of inverse B-decay, *Astrophys. J.*, **383**, p. 745.

Landau, L. D. and Lifshitz, E. M. (1977), *Quantum Mechanics*, Pergamon Press, ISBN 978-0750635394.

Lopes, L. and Menezes, D. P. (2015), Stability window and mass-radius relation for magnetized strange quark stars, *J. Cosmol. Astropart. Phys.*, **8**(002).

Miller, M., Lamb, F., Dittmann, A., Bogdanov, S. and et al (2019), PSR J0030+0451 Mass and Radius from *NICER* Data and Implications for the Properties of Neutron Star Matter, *Astrophys. J. Lett.*, **887**(1), p. 24.

Mukhopadhyay, S., Atta, D. and Basu, D. N. (2017), Landau quantization and mass-radius relation of magnetized white dowarfsin general relativity, *Rom. Rep. Phys.*, **69**(101).

Nurmamat, N., Zhu, C., Lul, G., Wang, Z., Li, L. and Liu, H. (2019), Quark novae: An alternative chanel for the formation of isolated milisecond pulsars, *J. Astrophys. Astron*, **40**(32).

Ouyed, R., Dey, J. and Dey, M. (2002), Quark-Novae, *Astron. Astrophys*, **390**(3), p. 512.

Ouyed, R., Leahy, D. and Koning, N. (2015), Hints of a second explosion (a quark nova) in Cassiopeia A Supernova, *Res. Astron. Astrophys*, **15**(483).

Ouyed, R. and Staff, J. E. (2013), Quark-novae in neutron star - white dwarf binaries: a model for luminous (spin-down powered) sub-Chandrasekhar-mass Type Ia supernovae?, *Res. Astron. Astrophys*, **13**(4), p. 435.

Riley, T. E., Watts, A. L., Bogdanov, S. and et al (2019), A *NICER* View of PSR J0030+0451: Millisecond Pulsar Parameter Estimation, *Astrophys. J. Lett.*, **887**(1), p. 21.

Tews, I., Margueron, J. and Reddy, S. (2018), Critical examination of constraints on the equation of state of dense matter obtained from GW170817, *Phys. Rev. C*, **98**(4).

Zhao, X. F. (2015), The properties of the massive neutron star PSR J0348+0432, *Int. J. Mod. Phys. A*, **24**(08), p. 1550058.